The KH-type RNA-binding protein PSI is required for *Drosophila* viability, male fertility, and cellular mRNA processing

Emmanuel Labourier, Marco Blanchette, Jennie W. Feiger,[1] Melissa D. Adams,[2] and Donald C. Rio[3]

Department of Molecular and Cell Biology, University of California, Berkeley, California 94720, USA

Direct interactions between RNA-binding proteins and snRNP particles modulate eukaryotic pre-mRNA processing patterns to control gene expression. Here, we report that the conserved U1 snRNP-interacting RNA-binding protein PSI is essential for *Drosophila* viability. A null PSI mutation is recessive lethal at the first-instar larval stage, and lethality is fully rescued by transgenes expressing the PSI protein. A mutant transgene that lacks the PSI–U1 snRNP-interaction domain restores viability but shows courtship behavior abnormalities and meiosis defects during spermatogenesis, resulting in a complete male sterility phenotype. Using cDNA microarrays, we have identified specific target mRNAs with altered expression profiles in these mutant males. A subset of these transcripts is also found associated with PSI in endogenous immunopurified ribonucleoprotein complexes. One specific target, the *hrp40/squid* transcript, shows an altered pre-mRNA splicing pattern in PSI mutant testes. We conclude that a functional association between the PSI protein and the spliceosomal U1 snRNP particle is required for normal *Drosophila* development and for the processing of specific PSI-interacting cellular transcripts. These results also validate the use of cDNA microarrays to characterize in vivo RNA-processing defects and alternative pre-mRNA splicing patterns.

[*Key Words*: Pre-mRNA splicing; U1 snRNP 70K; microarray; spermatogenesis; *Drosophila*]

Received September 27, 2001; revised version accepted November 9, 2001.

The posttranscriptional regulation of gene expression is a complex and critical process for all eukaryotic cells. RNA metabolism requires a large number of protein factors and intimate coordination among the transcription, capping, splicing, and polyadenylation machineries; and is regulated by a variety of signaling pathways (Hirose and Manley 2000). In metazoans, which necessitate a qualitative and quantitative control of gene expression according to developmentally, sex-specific, or tissue-specific cues, the processing of messenger RNA precursors (pre-mRNA) represents a powerful and versatile regulatory mechanism (Black 2000; Smith and Valcarcel 2000; Graveley 2001). RNA-binding proteins play a critical role in this process because they are involved in all aspects of RNA metabolism including nuclear processing, nucleo–cytoplasmic export, stability, and translation initiation.

In the fruit fly, *Drosophila melanogaster*, an elegant example of tissue-specific pre-mRNA processing regulation has been provided by studies on the *P*-element transposase. The RNA-binding protein *P*-element somatic inhibitor (PSI) specifically binds to the *P*-element pre-mRNA (Siebel et al. 1994) and is required for the soma-specific inhibition of *P*-element pre-mRNA third intron splicing in vitro and in vivo (Siebel et al. 1994, 1995; Adams et al. 1997). PSI contains four N-terminal hnRNP K-homology (KH) RNA-binding domains, and its C terminus is rich in the amino acids glycine, glutamine, and alanine (Siebel et al. 1995). The same modular organization is found in hypothetical *Caenorhabditis elegans* proteins (The *C. elegans* Sequencing Consortium 1998) and in a related family of mammalian proteins known as the fuse binding proteins (FBP/KSRP; Davis-Smyth et al. 1996; Min et al. 1997). FBP2/KSRP has been shown to modulate the neural-specific inclusion of the alternatively spliced N1 exon of the human *src* pre-mRNA (Min et al. 1997), and FBP, first identified as a single-stranded DNA-binding protein in the c-*myc* gene region (Duncan et al. 1994), has been proposed to bind and regulate *GAP43* mRNA stability during neuronal differentiation (Irwin et al. 1997). PSI and its metazoan orthologs all possess one to three repeats of a short, highly conserved, tyrosine-rich motif within their C-terminal region. The two PSI repeats, the so-called A and B motifs (Siebel et al. 1995), are necessary and sufficient to mediate a direct association of PSI with the spliceosomal U1 small nuclear ribonucleoprotein (U1 snRNP) particle in *Drosophila* Kc cell nuclear extracts (Labourier et al.

Present addresses: [1]GenRISK Program, Cedars-Sinai Medical Center, Los Angeles, CA 90048, USA; [2]Department of Biology, University of North Carolina, Chapel Hill, NC 27599, USA.
[3]Corresponding author.
E-MAIL don_rio@uclink4.berkeley.edu; FAX (510) 642-6062.
Article and publication are at http://www.genesdev.org/cgi/doi/10.1101/gad.948602.

2001). This interaction modulates U1 snRNP binding on the *P*-element third intron 5′ splice site and its upstream exonic regulatory element in vitro, providing a mechanistic explanation for the soma-specific regulation of *P*-element pre-mRNA splicing.

Although RNA-binding proteins have been shown to influence the RNA-processing machinery either positively or negatively by direct interactions with U1 snRNP particles (Eperon et al. 1993, 2000; Kohtz et al. 1994; Lou et al. 1998; Forch et al. 2000; Spingola and Ares 2000; Labourier et al. 2001), little is known about their functional relevance in vivo. Furthermore, it has been difficult to identify the specific target pre-mRNA interacting with and regulated by these factors in *Drosophila* (Kanaar et al. 1993; Ring and Lis 1994; Rudner et al. 1996). In this work, we have investigated the role of the full-length PSI protein and its C-terminal AB motif in *Drosophila* development. We report that PSI is a nuclear protein widely expressed throughout fly development and required for viability. A null PSI mutation causes lethality at the first-instar larval stage. Rescue experiments with wild-type or mutant *PSI* transgenes show that PSI, through its AB motif, interacts directly with U1 snRNP particles and plays a critical role in meiosis during spermatogenesis. Using a combination of genetic, genomic, and biochemical experiments, we show that the association of PSI with U1 snRNP is required to regulate the expression of specific PSI-interacting cellular mRNA in vivo. These results illuminate the function of PSI outside the context of *P*-element splicing regulation, genetically link the PSI–U1 snRNP interaction to differentially expressed target transcripts, and provide a general foundation for understanding how KH-type RNA-binding proteins can modulate metazoan development and RNA-processing patterns in a tissue- or sex-specific manner.

Results

PSI *is an essential gene*

To test the effect of a loss of PSI activity in *Drosophila*, mutations in the gene encoding PSI were generated. A reverse genetic approach, allowing the isolation in the heterozygous state of potentially recessive lethal mutations, was undertaken using the *P*-element insertion strain l(2)k05207. After two local *P*-element transposition/excision screens, one strain lacking the 5′ third of the *PSI* coding sequence and its promoter was identified by DNA sequence analysis of genomic PCR products (Fig. 1A; see Materials and Methods). Analysis of this mutant, called *v16*, indicated that the deletion is homozygous lethal at the first-instar larval stage and is null for the PSI protein (Fig. 1B). No obvious pattern defects or cuticular phenotypes were observed in homozygous *v16* embryos (data not shown).

To determine whether the *v16* deletion only affects PSI expression, *P*-element-mediated germ-line transformation with three different *PSI* transgene constructs was performed to rescue the *v16* lethal phenotype (Fig. 1C). Four independent transformant lines containing a 10.6-kb DNA genomic fragment encompassing the *PSI* locus completely restored the viability of the *v16* mutant. In contrast, no complementation was observed with five independent lines carrying a frameshift mutation within the *PSI* coding region of the genomic transgene, showing

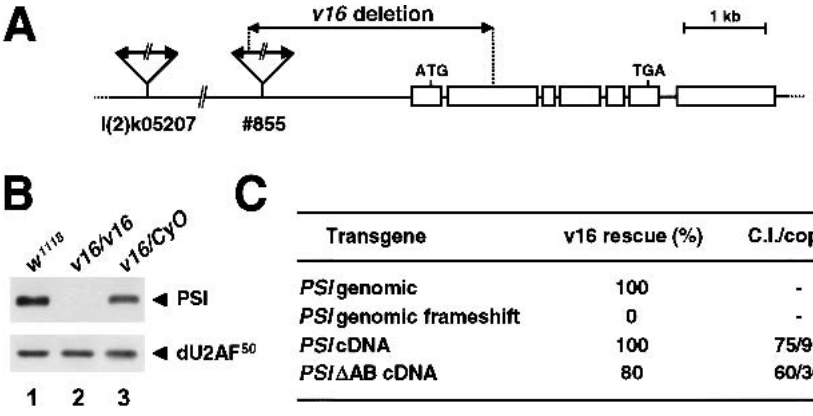

Transgene	v16 rescue (%)	C.I./cop. (%)
PSI genomic	100	-
PSI genomic frameshift	0	-
PSI cDNA	100	75/95
*PSI*ΔAB cDNA	80	60/30

Figure 1. Isolation and complementation analysis of the *v16* mutation. (*A*) The strain l(2)k05207, carrying a *P[lacW]* transgene at the cytological position 53D13-15, was used in a local hopping screen to isolate the strain #855, which contains a new *P* element inserted ~2 kb upstream of the *PSI* coding sequence. Both *P* elements were removed by a two-step excision screen to generate the null *v16* strain. PCR analyses of this line showed that the PSI-distal 3′ end of the *P*-element #855 was intact (nt 9360–10691) and that the *PSI* 5′ UTR and coding sequence have been deleted up to nucleotide 821. (*B*) Protein extracts prepared from w^{1118}, homozygous *v16*, or balanced *v16* first-instar larvae were resolved on a 10% SDS-polyacrylamide gel, transferred to nitrocellulose, and analyzed by immunoblotting using polyclonal antibodies specific for PSI (*top* panel) or the large subunit of *Drosophila* U2 snRNP Auxiliary Factor ($dU2AF^{50}$) as a loading control (*bottom* panel). (*C*) Rescue of the *v16* recessive lethal phenotype by *PSI* or *PSIΔAB* transgenes. Virgin females balanced for the *v16* mutation and carrying one copy of the various independent *P[w⁺;PSI]* insertions on the X or third chromosome (*P[w⁺;PSI]/w;v16/CyO;+/+* or *w/w;v16/CyO;P[w⁺;PSI]/+*) were crossed with males *w/Y;v16/SM6β;+/+*. Percentages of rescue, determined by scoring the balanced and unbalanced progeny carrying *P[w⁺;PSI]*, ranged from 90% to 116% with the *PSI* genomic or cDNA transgenes and 68% to 85% with the *PSIΔAB* cDNA transgenes. No rescue was observed with a genomic transgene carrying a frameshift mutation 132 nt downstream of the *PSI* ATG codon. Approximately 1000 progeny were scored for each cross. For behavioral tests, individual mature males (4 days old, $n = 50$) were presented with a wild-type virgin female into a cylindrical mating chamber, and the courtship behavior of the pair was monitored until they copulated, or for 30 min, whichever occurred first. (C.I.) Fraction of the observation period during which the male performed any courtship activity; (cop.) fraction of the observed males that actually copulated.

that the rescue is specific for expression of PSI. Finally, an in vivo PSI expression vector, containing the *PSI* cDNA flanked by the natural *PSI* promoter, 5′- and 3′-UTR genomic sequences, rescued the *v16* mutation as efficiently as the genomic construct. Rescued transgenic flies were healthy, and stocks homozygous for the *v16* mutant allele could be maintained in the presence of the *PSI* transgene. We conclude that the null *v16* mutation is recessive lethal and that PSI has a crucial cellular function(s) required for *Drosophila* viability.

The PSI AB motif is required in vivo

The C-terminal AB motif of PSI mediates a direct interaction between PSI and U1 snRNP particles in *Drosophila* Kc cell nuclear extracts (Labourier et al. 2001). To test the requirement of this motif for *Drosophila* viability and development, a construct encoding a PSI protein lacking only the A and B repeats was engineered, and germ-line transformants were tested for rescue of the *v16* mutant phenotype. Surprisingly, all of the independent transgenic lines isolated could restore the viability (*PSIΔAB* cDNA, Fig. 1C). However, stocks homozygous for the *v16* mutant allele could not be maintained in the presence of the mutant Δ*AB* transgene. Males *v16;P[PSIΔAB]* were ~10% smaller than their heterozygous siblings or males rescued by the full-length *PSI* cDNA transgene. Interestingly, the *v16;P[PSIΔAB]* males were completely sterile.

Because several mutations affecting courtship behavior have been shown to alter male fertility in *Drosophila* (Hall 1994; Orgad et al. 1997), we next analyzed the reproductive activity of the *v16;P[PSIΔAB]* mutant males. Although all the sequential steps of the courtship ritual were observed in standard single-pair mating behavioral tests (orienting toward and following the female, wing extension and vibration, licking the female's genitalia, tapping the female's abdomen, and attempts to copulate), abnormal periods of lack of interest for receptive w^{1118} or Canton-S virgin females were recorded. The courtship index (C.I.) representing the fraction of the observation time that each male actually spent courting was 75% for *v16;P[PSI]* males and 60% for *v16;P[PSIΔAB]* males (Fig. 1C). Furthermore, only 30% of the mutant *v16;P[PSIΔAB]* mature males eventually copulated over a 30-min observation time period (~95% for w^{1118} or *v16;P[PSI]* males; Fig. 1C), yet these matings yielded no progeny. After copulation, no sperm were stored in the female seminal receptacle and spermatheca, suggesting that these males were also defective in producing mature sperm.

Spermatogenesis is defective in v16;P[PSIΔAB] *mutants*

During *Drosophila* spermatogenesis, each primary spermatogonial cell generates 16 spermatocytes after four gonial mitotic divisions. Two consecutive meiotic divisions result in a cyst containing 64 haploid spermatids, which remain connected by cytoplasmic bridges throughout differentiation and maturation (Fuller 1993). Microscopic examination of dissected testes from *v16;P[PSI]* males showed a normal arrangement of bundles of elongating spermatids leading to accumulation of mature motile sperm in the seminal vesicle (Fig. 2A, panels I and IV). In contrast, two slightly different but fully penetrant phenotypes were observed in *v16;P[PSIΔAB]* males, depending on the chromosomal insertion sites of the *PSIΔAB* transgene used for the rescue experiment. In two-thirds of the lines examined, spermatid cysts were disorganized and spermatid bundles were intermingled (Fig. 2A, cf. panels I and III). The postmeiotic onion-stage early spermatids were often multinucleate and contained atypical large mitochondrial derivatives, suggesting that the meiotic divisions were defective. Abnormal spermatids started to differentiate but failed to mature, and no sperm were stored in the seminal vesicle (Fig. 2A, panel VI). In other independent transgenic lines, almost no postmeiotic cells were observed. No bundles of spermatids were formed, and large cells similar to undifferentiated premeiotic spermatocytes filled the testes (Fig. 2A, panels II and V).

Immunostaining of male germ-line cell cytoplasm using anti-vasa antibodies (Lasko and Ashburner 1990) showed that the mitotic divisions of the primary spermatogonial cells occurred normally in both *v16;P[PSI]* and *v16;P[PSIΔAB]* testes (Fig. 2B). Cysts of spermatogonial cells and a clear spermatogonia/spermatocyte transition, evidenced by DAPI staining, were observed. Furthermore, cysts of 16 large mature spermatocytes were easily discernable in testes from w^{1118} (data not shown) or *v16;P[PSI]* (Fig. 2B, panel V) males. The spermatocyte/spermatid transition was also evident in *v16;P[PSI]* males as no other vasa-positive cells were detected in the testes (Fig. 2B, panel I). In contrast, a strong staining was observed throughout the *v16;P[PSIΔAB#1]* testes (Fig. 2B, panels II and VI), confirming an accumulation of mature primary spermatocytes at the expense of the postmeiotic cells. Although we can not rule out the existence of other more subtle abnormalities in *v16;P[PSIΔAB]* males or females, these data show that the lack of PSI AB motif in vivo affects meiosis during spermatogenesis, resulting in male sterility. The observation that *v16;P[PSIΔAB]* males court poorly suggests that this loss-of-function phenotype is pleiotropic and may also affect the nervous system.

PSIΔAB expression and localization in v16;P[PSIΔAB] *mutants*

Given the striking functional differences of the PSI and PSIΔAB proteins in vivo, we were interested in determining whether there were any differences in their expression levels and/or stability. Immunoblot analysis of whole-fly protein extracts showed that the levels of PSI or PSIΔAB expression in the rescued homozygous *v16* lines were equivalent to the heterozygous balanced *v16* strain or the original w^{1118} transformation host strain (Fig. 3B). Furthermore, no difference in the level of *PSIΔAB* transgene expression was detected between the

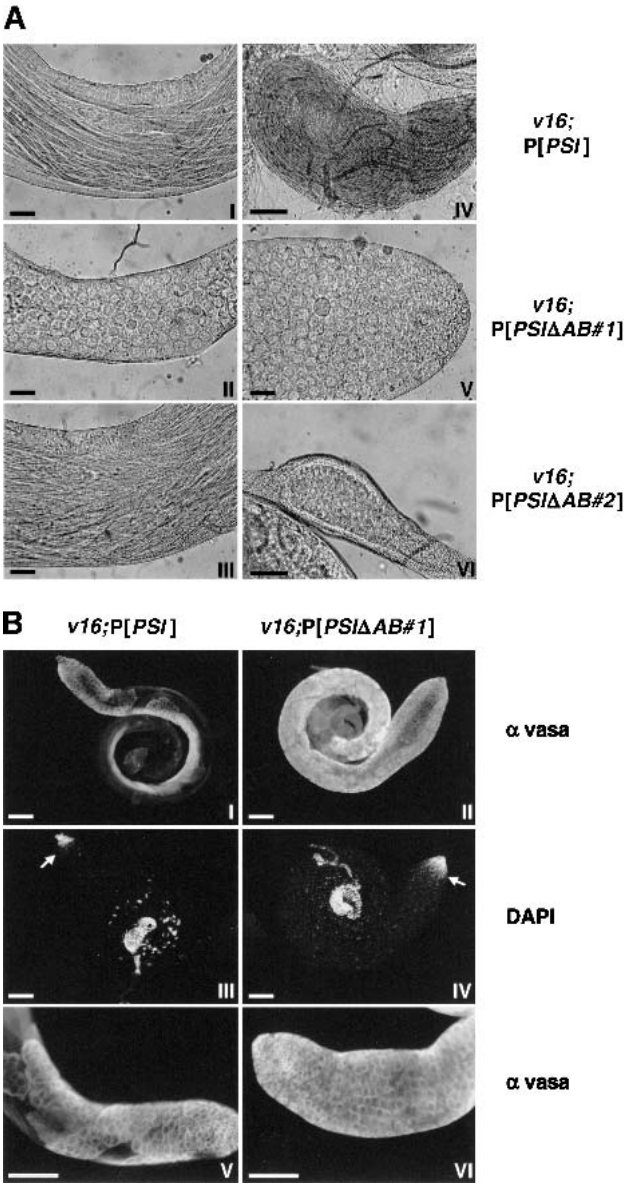

Figure 2. Spermatogenesis is defective in *v16;P[PSIΔAB]* adult males. (*A*) Light micrographs of testes dissected from homozygous *v16* adult males rescued by the *PSI* (*I*,*IV*) or two independent *PSIΔAB* (*II*,*III*,*V*,*VI*) cDNA transgenes. Shown are the central part of mature testes (*I*,*II*,*III*), the apical tip of a testis *v16;P[PSIΔAB#1]* (*V*) or seminal vesicles with (*IV*) and without (*VI*) accumulation of mature motile sperm. Scale bar, 25 µm. (*B*) Testes from rescued *v16;P[PSI]* (*I*,*III*,*V*) or *v16;P[PSIΔAB#1]* (*II*, *IV*,*VI*) adult males were fixed and stained with anti-vasa rabbit antibodies and Alexa Fluor secondary antibodies (*I*,*II*,*V*,*VI*) and with DAPI (*III*,*IV*).The bright DNA stain is restricted to the apical tip of the testes as spermatocytes and postmeiotic cells fluoresce more weakly owing to chromatin reorganization. The spermatogonia/spermatocyte transition is indicated by arrows. Detail of the apical end of testes showing the cytoplasmic localization of the vasa protein and cysts of spermatocytes or spermatogonial cells (*V*,*VI*). Scale bar, 100 µm.

sterile *v16;P[PSIΔAB]* males and their fertile rescued sisters (data not shown). In situ hybridization using a digoxygenin-labeled anti-sense RNA probe and immunostaining of whole-mount embryos using affinity-purified polyclonal antibodies confirmed that both the *PSI* and *PSIΔAB* transcripts and proteins have the same pattern of expression and localization in vivo (Fig. 3C; data not shown). With the exception of the embryonic pole cells, the endogenous PSI protein, as well as the transgenic PSI and PSIΔAB proteins, were detected in all somatic cell nuclei throughout embryonic development. As shown below, PSI and PSIΔAB also localize to the nucleus in adult tissues. We conclude that the absence of the AB motif does not affect the subcellular distribution or stability of the PSIΔAB protein.

Lack of the PSI–U1 snRNP interaction in v16;P[PSIΔAB] *mutants*

We next asked whether PSIΔAB could interact with endogenous U1 snRNP particles in flies homozygous for the *v16* mutation and rescued by the *PSIΔAB* cDNA transgene. Nuclear extracts were prepared from w^{1118}, *v16;P[PSI]*, or *v16;P[PSIΔAB]* embryos, and U1 snRNP particles were isolated using a biotinylated 2′-*O*-methyl anti-sense U1 snRNA oligonucleotide (Labourier and Rio 2001). Immunoblot analysis of affinity-selected U1 snRNP fractions indicated that PSI is associated with U1 snRNP particles in w^{1118} and *v16;P[PSI]* embryonic nuclear extracts (Fig. 3D, lanes 1–6). In contrast, no PSIΔAB protein was detected in the U1 snRNP fraction purified from the *v16;P[PSIΔAB]* nuclear extract (Fig. 3D, lane 8). Hybridization of the affinity-selected RNA species with an anti-sense U1 snRNA riboprobe confirmed that U1 snRNP particles were efficiently purified from both extracts (data not shown).

Previous studies have shown that PSI interacts directly with the C-terminal arginine–serine-rich (RS) domain of the U1 snRNP-specific 70K protein (dU1–70K) in Drosophila Kc cell nuclear extracts (Labourier et al. 2001). Glutathione-S-transferase (GST) fusion protein interaction assays confirmed that both the full-length dU1–70K protein and a C-terminal dU1–70K fragment (GST-dU1–70K or GST-dU1–70K 189–448; Mancebo et al. 1990; Labourier et al. 2001) can efficiently retrieve the PSI protein present in w^{1118} or *v16;P[PSI]* embryonic nuclear extracts, whereas the PSIΔAB protein was not selected from *v16;P[PSIΔAB]* extracts (data not shown). No PSI or PSIΔAB protein was detected when the GST protein alone or a fusion protein containing the N-terminal RRM-type RNA-binding domain of dU1–70K (GST-dU1–70K 1–188; Mancebo et al. 1990; Labourier et al. 2001) was used (data not shown). Taken together, these results show that the PSI AB motif is required for a direct interaction with the C-terminal RS domain of dU1–70K in *Drosophila*.

Alteration of mRNA expression profiles in v16;P[PSIΔAB] *mutants*

Our genetic and biochemical experiments both suggest that one of the crucial cellular PSI functions may be to

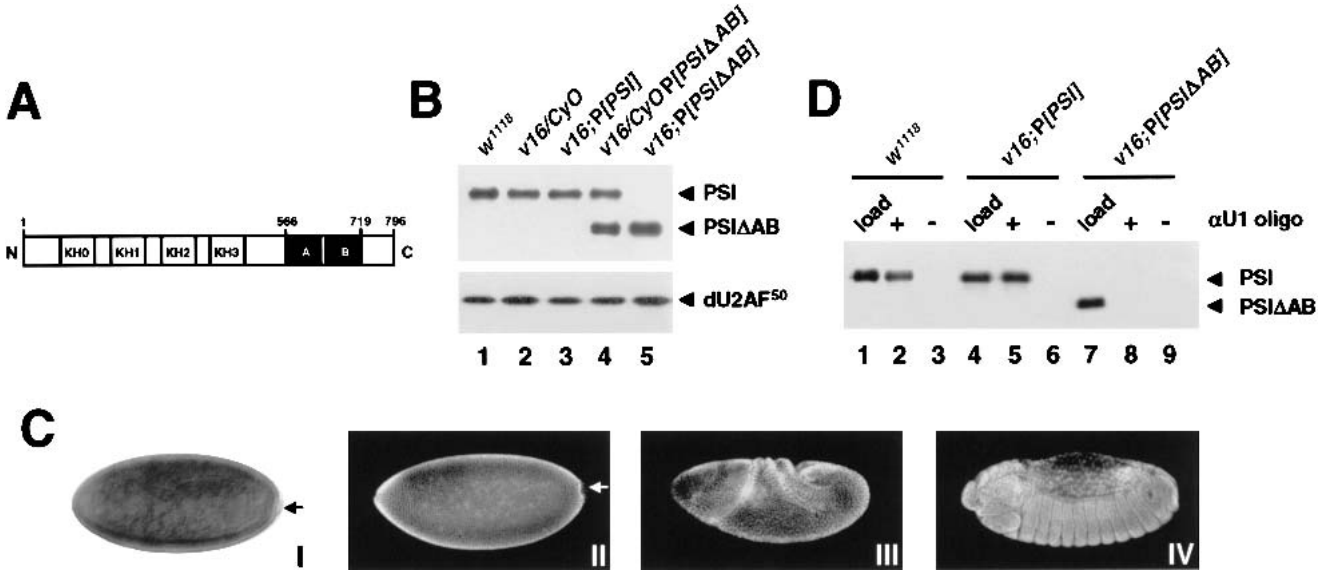

Figure 3. Analysis of *PSI* and *PSIΔAB* transgene products. (*A*) Schematic representation of the PSI domain structures. The KH-type RNA-binding domains (KH0–KH3) and the protein–protein interaction motifs (repeats A and B) are boxed in white and black, respectively. The PSIΔAB protein lacks amino acids 566–719. (*B*) Immunoblot analyses of whole-fly protein extracts prepared from w^{1118} males (lane *1*) or transgenic males balanced (lanes *2,4*) or homozygous for the *v16* mutation (lanes *3,5*) and carrying a *PSI* (lane *3*) or *PSIΔAB* (lanes *4,5*) cDNA transgene were performed as in Figure 1B. (*C*) Stage 4 w^{1118} (*I,II*), stage 8 *v16;P[PSI]* (*III*), or stage 14 *v16;P[PSIΔAB]* (*IV*) embryos were fixed and hybridized with a digoxygenin-labeled anti-sense *PSI* RNA probe (*I*) or stained with affinity-purified anti-PSI polyclonal antibodies and Alexa Fluor secondary antibodies (*II–IV*). No staining was detected in the pole cells (arrows). Identical patterns of expression were observed in w^{1118}, *v16;P[PSI]*, and *v16;P[PSIΔAB]* embryos. (*D*) PSI–U1 snRNP interaction in embryonic nuclear extracts. Embryonic nuclear extracts, prepared using 0–12-h w^{1118} (lanes *1,2*), *v16;P[PSI]* (lanes *3,4*), or *v16;P[PSIΔAB]* (lanes *5,6*) embryos were incubated in the absence (–) or presence (+) of a biotinylated 2′-*O*-methyl anti-sense U1 snRNA oligonucleotide. U1 snRNP particles affinity-selected on streptavidin-agarose beads were resolved on a 10% SDS-polyacrylamide gel, transferred to nitrocellulose, and analyzed by immunoblot using affinity-purified anti-PSI polyclonal antibodies. To show that the level of PSI or PSIΔAB protein expression in rescued *v16* embryos is equivalent to the normal level of PSI expression in w^{1118} embryos, 1/50 of the input nuclear extracts were analyzed in parallel (load; lanes *1,4,7*).

interact with U1 snRNP and to modulate its activity on a variety of endogenous pre-mRNAs. To identify putative PSI-regulated target transcripts in vivo and to determine whether their processing might be altered by a loss of PSI–U1 snRNP association, the pattern of mRNA expression in males homozygous for the *v16* mutation and rescued either by the wild-type *PSI* or *PSIΔAB* transgene was compared using high-density cDNA microarrays. We reasoned that if specific transcripts are incorrectly processed in *v16;P[PSIΔAB]* males, resulting in processing or stability defects, then these changes might be detected by differential hybridization to individual cDNAs of known sequences. Although not specifically designed to detect pre-mRNA splicing changes, these *Drosophila* cDNA expressed sequence tag (EST) microarrays were useful to identify RNA-processing defects (see below).

PolyA$^+$ RNA samples were purified from *v16;P[PSI]* or *v16;P[PSIΔAB]* males, and the corresponding cDNAs, labeled, respectively, with Cy3 or Cy5 fluorescent dyes, were mixed and hybridized to microarrays carrying 6300 spotted *Drosophila* EST clones. Collected data were individually filtered and normalized (see Materials and Methods) and used to generate a database containing a calculated differential expression factor for all the genes that were reproducibly and qualitatively detected in independent experiments (Table 1; http//riodata.berkeley.edu). In this format, a value below –1 indicates a reduction in the level of expression of a given mRNA in *v16;P[PSIΔAB]* males. A value above +1 indicates an increase. Analysis of this set of data showed that <2% of the 5150 unique genes present on the arrays displayed a significant differential expression (Fig. 4A). Reproducible results were obtained in nine independent experiments (Table 1). In addition, ~400 ESTs were printed in duplicate on each microarray and behaved the same way, further showing the consistency of the results (see, e.g., *CG17754*, *CG1479*, and *CG18242* in Table 1).

PSI interacts with specific mRNAs altered in v16;P[PSIΔAB] *mutants*

A second approach to characterize potential PSI-regulated targets was to ask whether PSI differentially associates with specific mRNAs in endogenous ribonucleoprotein complexes. PSI-interacting RNA were identified by large-scale immunoaffinity purification using anti-PSI polyclonal antibodies (M. Blanchette and D.C. Rio, unpubl.) and hybridization to *Drosophila* cDNA microarrays. Analysis of five independent microarrays allowed us to characterize the transcripts that were reproducibly

Table 1. *Top 50 differentially expressed transcripts (mRNA profiling)*

Gene	Name	Ratio[a]	SD[a]	*n*	Molecular information/function
CG5857		4.90	0.68	9	unknown function
CG10390	***Taf60-2***	4.68	1.67	8	transcription initiation
CG11334		3.43	0.43	9	translation initiation
CG6790		3.09	0.36	9	GPI anchor synthesis
CG6306		2.93	0.37	9	unknown function
CG18316		2.88	0.89	9	unknown function
CG17754		2.77	0.94	9	related to Kelch, a ring canal actin organizer
CG17754		2.72	0.80	9	related to Kelch, a ring canal actin organizer
CG4178	*Lsp1*β	2.68	1.52	9	glutamine amidotransferase
CG4463	*Hsp23*	2.48	1.65	8	CNS- and testis-specific in unstressed flies
CG5704		2.47	0.19	9	esterase/lipase, related to kraken
CG11703		2.41	0.43	9	sodium/potassium ATPase
CG10138	*PpD5*	2.41	0.68	6	serine/threonine phosphatase
CG1340		2.19	0.55	9	RNA binding,translation initiation
CG12101	***Hsp60***	2.18	0.76	9	mitochondrial chaperone in unstressed flies
CG1898		2.15	0.57	9	translation termination
CG11654	*Ahcy13*	2.08	0.55	9	adenosylhomocysteinase
CG10800	*Rca1*	2.08	1.25	7	cell cycle, role during neurogenesis
CG5654	***yps***	–1.90	0.47	9	RNA binding, role in mRNA localization
CG1479	*bt*	–1.78	0.81	9	projectin, serine/threonine kinase
CG1479	*bt*	–2.00	0.88	9	projectin, serine/threonine kinase
CG3291	*pcm*	–2.02	0.62	8	5′-3′ exoribonuclease
CG7157	*Acp36DE*	–2.02	0.65	9	seminal prohormone, role in sperm storage
CG12606	*nAcR-64B*	–2.04	0.51	7	neurotransmitter receptor
CG10248	*Cyp6a8*	–2.05	0.53	9	mitochondrial cytochrome P450
CG7178	*wupA*	–2.07	0.64	9	troponin I
CG10811	*eIF-4G*	–2.10	0.68	9	translation initiation
CG2139	*aralar1*	–2.11	0.52	9	mitochondrial carrier
CG13431	*MGAT1*	–2.13	0.54	8	acetylglucosaminyltransferase
CG14032	*Cyp4ac1*	–2.13	0.40	9	mitochondrial cytochrome P450
CG1691	*Imp*	–2.17	0.70	9	RNA binding, role in axon guidance
CG17791	***sqd***	–2.27	0.47	9	RNA binding, role in mRNA localization
CG11804	*ced-6*	–2.38	0.82	9	signal transduction
CG1587	*Crk*	–2.45	0.60	9	SH3/SH2 adaptor, signal transduction
CG5670	*Atp*α	–2.47	0.50	9	sodium/potassium ATPase
CG7981	*pcan*	–2.50	0.46	9	cell adhesion
CG6320	*Ca*-β	–2.51	0.41	9	voltage-dependent calcium channel
CG17704	*Nipped-B*	–2.52	0.68	8	chromosome condensation, DNA repair
CG11059	*calsyntenin*	–2.53	0.49	9	cell adhesion, role in synaptic transmission
CG1838	*myoglianin*	–2.62	0.58	9	TGF-β, signal transduction
CG17436	*Rad21*	–2.82	0.71	9	chromosome condensation, DNA repair
CG1507	*Pur-*α	–2.83	0.39	9	single-stranded DNA binding, transcription
CG5887	***desat1***	–2.85	0.58	9	desaturase, role in pheromone synthesis
CG10392	*Ogt*	–2.92	0.67	9	acetylglucosaminyltransferase
CG17759	*Gα49B*	–3.33	0.52	9	G protein, signal transduction
CG11081	***plexA***	–3.57	0.57	9	semaphorin receptor, role in axon guidance
CG18242		–3.66	0.77	7	related to titin
CG18242		–3.69	1.11	9	related to titin
CG6357		–4.27	0.61	9	similar to cathepsin, a cysteine proteinase
CG4784		–4.92	1.68	9	related to cuticular structural proteins

[a]Calculated for *n* independent experiments.
Boldface indicates gene mentioned in text.

present in PSI-containing ribonucleoprotein particles isolated from Canton-S embryonic nuclear extracts (Fig. 4A; Table 2). Interestingly, ~20% of these transcripts, such as *yps*, *Hsp60*, and *desat1*, were also differentially expressed in *v16;P[PSIΔAB]* males (Table 2). RT–PCR experiments confirmed that these mRNAs are highly enriched in immunopurified PSI fractions but not in control immunopurifications using total rabbit IgG and embryonic nuclear extracts (Fig. 4B). In addition, each of the tested mRNAs showed the expected three- to twofold increased (*Taf60-2* and *Hsp60*) or decreased (*yps*, *desat1*, and *plexA*) level of expression in *v16;P[PSIΔAB]* sterile males versus *v16;P[PSI]* wild-type males (Fig. 4C). As no variation was observed for other control mRNAs (Fig. 4D; data not shown), we conclude that the loss of PSI–U1snRNP interaction in *v16;P[PSIΔAB]* males can result

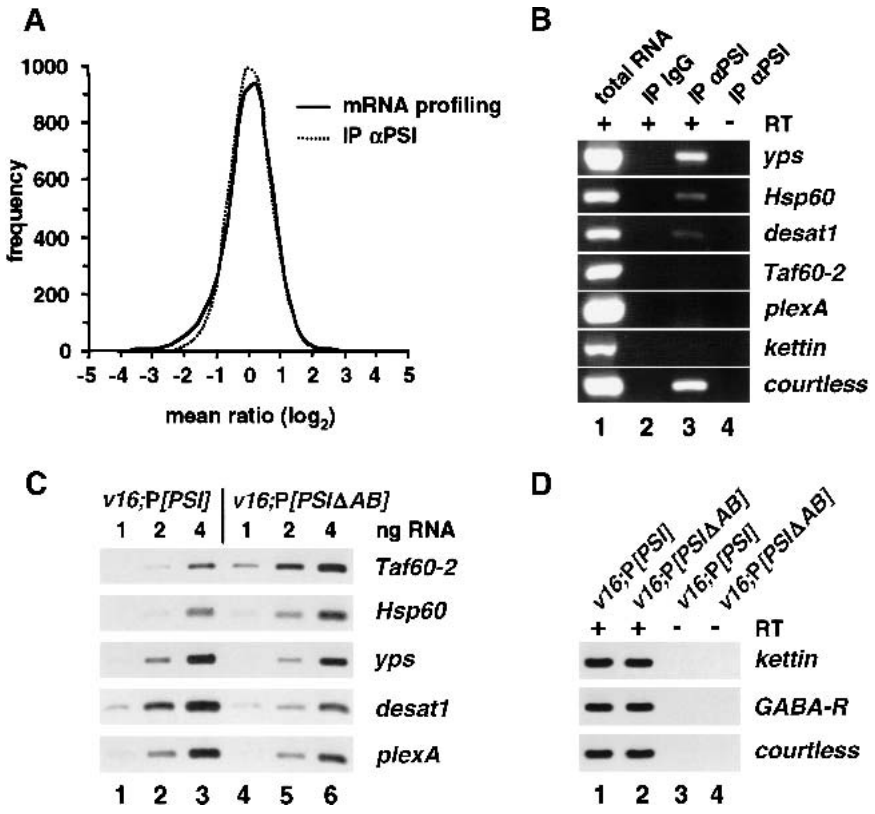

Figure 4. Expression patterns of specific PSI-interacting transcripts are affected in *v16;P[PSIΔAB]* mutants. (*A*) Smoothened distributions of mean ratios calculated using normalized data from *n* independent microarray experiments. Distributions for the *v16;P[PSIΔAB]* versus *v16;P[PSI]* differential expression experiments (mRNA profiling; adult male RNA samples; $n = 9$) and for the PSI-interacting experiments (IP αPSI; embryonic RNA samples; $n = 5$) are both centered and normal-like. (*B*) Total RNA purified from 0–12-h embryos (~100 ng, lane *1*) or 1/250 of the RNA immunopurified from 1 mL of embryonic nuclear extract using total rabbit IgG (lane *2*) or affinity-purified anti-PSI polyclonal antibodies (lane *3*; ~8 ng of RNA) were analyzed by RT–PCR with (+) or without (–) reverse transcription step and PCR primers specific for the indicated cDNA. PCR products were resolved on 1% agarose gels and stained with ethidium bromide. (*C*) Quantitative RT–PCR reactions using 1 ng (lanes *1,4*), 2 ng (lanes *2,5*), or 4 ng (lanes *3,6*) of polyA$^+$ RNA purified from *v16;P[PSI]* (lanes *1–3*) or *v16;P[PSIΔAB]* males (lanes *4–6*) and PCR primers specific for the indicated cDNA were resolved on 5% denaturing polyacrylamide gels and revealed by autoradiography. (*D*) Quantitative RT–PCR experiments were performed with (+) or without (–) reverse transcription step using 4 ng of polyA$^+$ RNA and PCR primers specific for *kettin* (giant muscle protein, titin family), *GABA-R* (receptor for the inhibitory neurotransmitter GABA, Rdl subunit), or *courtless* cDNA (ubiquitin-conjugating enzyme, see Discussion). PCR products were analyzed as in *C*.

in an incorrect processing of specific PSI-interacting transcripts.

The hrp40/squid *pre-mRNA splicing pattern is altered in* v16;P[PSIΔAB] *mutants*

Among the specific targets that were reproducibly highly ranked in both the mRNA profiling and PSI-interacting databases, our attention was drawn to *squid* (*CG17791*, Table 2). *squid* encodes a heterogeneous nuclear RNA-binding protein (hnRNP); a *squid* germ-line mutation causes female sterility (Kelley 1993). Furthermore, the *squid* pre-mRNA is alternatively spliced to produce three protein isoforms designated SqdA (hrp40.1), SqdS (hrp40.2), and SqdB (Fig. 5A) that perform different functions in the female germ line (Matunis et al. 1992; Kelley 1993; Norvell et al. 1999). Strikingly, the EST detected in our microarrays experiments (LD09564) was specific for the unspliced SqdA isoform.

RT–PCR analyses showed that the *SqdA* mRNA is the major form in embryonic extracts and is present in PSI-containing ribonucleoprotein complexes (Fig. 5B). In adult males, all of the three transcripts are expressed, although the *SqdA* mRNA is five times more abundant than *SqdB*, and the *SqdS* isoform is barely detectable (Fig. 5C, top panels). A significant reduction of expression in *v16;P[PSIΔAB]* males was observed only for the unspliced *SqdA* mRNA. By quantification of these PCR products, we determined that the spliced/unspliced (*SqdB*/*SqdA*) ratio increased by twofold in *v16;P[PSIΔAB]* males, suggesting that the PSIΔAB protein is less effective at inhibiting *SqdB* splicing. Similarly, a reduced level of *SqdA* mRNA expression, but not other control transcripts, was detected in testes dissected from *v16;P[PSIΔAB]* males (Fig. 5C, middle panels; data not shown). In contrast, the *squid* splicing profile was very different in the female germ line. RT–PCR analyses indicated that the accurately spliced SqdB isoform is highly expressed in ovaries dissected from *v16;P[PSI]* females (Fig. 5C, bottom panels). Consistent with the observation that *v16;P[PSIΔAB]* females do not exhibit oogenesis defects, no variation of the *SqdB*/*SqdA* ratio was detected between *v16;P[PSI]* and *v16;P[PSIΔAB]* ovaries. Taken together, these data suggest that a direct interaction between PSI and U1 snRNP particles is required in vivo for an efficient tissue-specific splicing inhibition of a subset of PSI-interacting transcripts such as the *hrp40/squid* pre-mRNA.

PSI is highly expressed in the male germ line

PSI was initially identified as a soma-specific pre-mRNA splicing factor, detected only at very low level in *Drosophila* ovaries by immunoblot analyses (Siebel et al.

Table 2. *PSI-interacting transcripts versus mRNA profiling*

		IP αPSI			mRNA profiling		
Gene	Name	Ratio	SD	*n*	Ratio	SD	*n*
CG7439		3.57	1.22	5	0.37	0.25	9
CG9381		3.14	1.08	5	–0.79	0.48	9
CG9281		3.05	0.69	5	0.96	0.72	8
CG5654	***yps***	2.66	0.97	5	–1.90	0.47	9
CG16747	*guf*	2.60	0.84	5	–0.78	0.51	9
CG5650	*Pp1-87B*	2.26	1.07	5	–0.25	0.37	9
CG12101	***Hsp60***	2.25	0.59	4	2.18	0.76	9
CG3943	*kraken*	2.13	0.23	4	1.39	0.39	9
CG17791	***sqd***	2.00	1.14	5	–2.27	0.47	9
CG7590	*scylla*	1.92	0.94	5	–0.92	0.40	9
CG15112	*enb*	1.90	0.56	5	0.59	0.37	9
CG17610	*grk*	1.88	0.86	4	–0.24	0.80	9
CG8293	*lap2*	1.88	0.32	5	1.29	0.26	9
CG12157	*Tom40*	1.87	0.58	5	1.27	0.44	9
CG1404	*ran*	1.78	0.83	5	1.46	0.75	9
CG4551	*smi35A*	1.62	0.54	5	0.89	0.42	9
CG1088	*Vha26*	1.60	0.80	5	–0.74	0.67	9
CG4084	*I(2)not*	1.60	0.67	5	1.47	0.33	9
CG7623	*sll*	1.59	0.54	5	0.62	0.44	7
CG1668	*Pbprp2*	1.55	0.61	4	–0.79	0.73	9
CG3644	*bic*	1.52	0.58	5	–0.02	0.19	9
CG3161	*Vha16*	1.49	0.1	4	0.25	0.38	8
CG12345	*Cha*	1.45	0.76	5	0.34	0.27	7
CG6575	*glec*	1.43	0.48	5	–0.38	0.46	8
CG1691	*Imp*	1.34	1.37	5	–2.17	0.70	9
CG5887	***desat1***	1.34	0.42	5	–2.85	0.58	9

Boldface indicates gene mentioned in text.

1995; Adams et al. 1997; Labourier et al. 2001). The above results prompted us to determine whether PSI is expressed in *Drosophila* testes. High levels of PSI and PSIΔAB proteins were detected by immunoblot analysis in testes dissected from w^{1118}, *v16;P[PSI]*, or *v16;P[PSIΔAB]* mature males (Fig. 6A). Immunostaining of whole-mount testes showed that both somatic and germ-line cells are stained by anti-PSI polyclonal antibodies at the apical end of w^{1118} (data not shown) or *v16;P[PSI]* adult testes (Fig. 6B, panel I). Only PSI-positive somatic cells were observed in the basal and central part of the testes as spermatids, and mature sperm did not stain. Expression of PSI in germ cells was further observed in w^{1118} or *v16;P[PSI]* males by double-labeling with anti-PSI and anti-vasa antibodies (data not shown), and in *v16;P[PSIΔAB#1]* males, where excess, premeiotic, vasa-positive spermatocytes were also strongly stained by anti-PSI antibodies throughout the testes (Fig. 6B, panel II). Importantly, both the PSI and PSIΔAB proteins were localized to the nucleus and expressed at high levels in somatic and germ-line cells (Fig. 6B, panels V and VI).

In contrast, the pattern of PSI expression in ovaries was very different. Only very low levels of PSI expression were detected by confocal imaging in the nuclei of the somatically derived follicle cells (Fig. 6C, panels I and II). A weak staining was also observed in nurse cell nuclei during the early stages of oogenesis. Consistent with this localization, in situ hybridization using a digoxygenin-labeled anti-sense RNA probe showed that the *PSI* mRNA is expressed in the nurse cell and early oocyte cytoplasm, as well as in the follicle cells surrounding the mature oocyte (Fig. 6C, panels III and IV). This pattern suggests that translation of *PSI* mRNA is down-regulated in the female germ line, because the level of PSI protein is low in nurse cells and oocytes. Furthermore, an FLP–DFS-induced germ-line clone analysis (Chou and Perrimon 1996) showed that PSI is not essential for oogenesis. *v16/v16* mosaic females laid embryos without obvious defects that developed into normal adult flies (data not shown). We conclude that unlike in the female gonad, PSI is highly expressed in the male germ line, where its function is required during spermatogenesis.

Discussion

This work provides several new insights into how RNA-binding proteins contribute to the control of gene expression patterns and the execution of underlying developmental programs in metazoans. First, we show that the KH-type RNA-binding protein PSI has a crucial cellular function required for *Drosophila* viability. PSI is a nuclear protein widely expressed throughout fly development, and a PSI null mutation is lethal at the first-instar larval stage. Second, we identify specific target transcripts that interact with and are regulated by PSI in vivo. Third, we show that the PSI C-terminal AB motif, which mediates the interaction of PSI with endogenous U1 snRNP particles, is essential for normal *Drosophila* development. Transgenic flies lacking the PSI AB motif exhibit a male sterility phenotype. Fourth, we present evidence that loss of the PSI–U1snRNP association affects the processing of a subset of PSI-interacting transcripts in vivo. These findings extend previous studies showing an involvement of PSI in the regulation of *P*-element transposase expression and clarify our understanding of the function(s) of KH-domain-containing proteins during metazoan development. Finally, our data also suggest that cDNA microarrays are powerful tools to study in vivo RNA-processing defects and alternative splicing patterns.

The *PSI* gene is unique in the *Drosophila* genome (Adams et al. 2000; Mount and Salz 2000). It therefore seemed likely that the loss of PSI expression in vivo would result in phenotypic consequences. The PSI null *v16* mutation is recessive lethal at the first-instar larval stage, and normal viability and development are fully restored by a PSI-encoding transgene. These results show that the *PSI* gene product has a crucial cellular function that is not redundant with other KH-type RNA-binding proteins. However, immunostaining experiments and observation of cuticle preparations did not reveal any obvious morphological defects in homozygous *v16* embryos. Similar loss-of-function phenotypes were reported previously for three other essential splicing factors, the large and small subunits of the U2 snRNP auxiliary factor (dU2AF^{50} and dU2AF^{38}; Kanaar et al. 1993), and the B52/SRp55 protein, a member of the SR protein family (Ring and Lis 1994). These widely expressed RNA-bind-

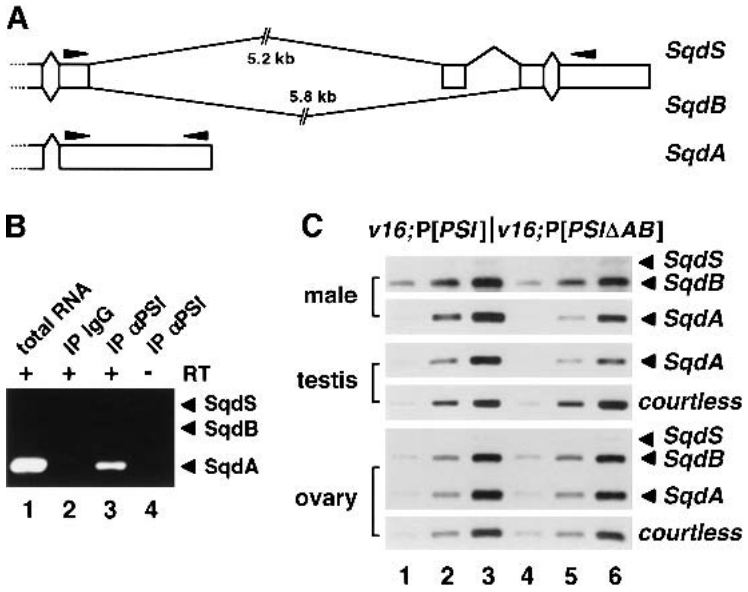

Figure 5. Analysis of the *hrp40/squid* pre-mRNA splicing pattern in *v16;P[PSIΔAB]* mutants. (*A*) Schematic diagram of the *Sqd* transcripts. Broken lines and open boxes represent intronic and cDNA sequences, respectively. The position of the PCR primers used in *B* and *C* is indicated by solid arrowheads. (*B*) RT–PCR reactions using embryonic RNA samples were performed and analyzed as in Figure 4B in the presence of three PCR primers to amplify all of the *sqd* transcripts. No *SqdB/S* isoforms were detected. (*C*) Quantitative RT–PCR experiments were performed as in Figure 4C with polyA$^+$ RNA isolated from adult males or 5, 10, and 20 ng of total RNA purified from testes or ovaries hand-dissected from *v16;P[PSI]* (lanes *1–3*) or *v16;P[PSIΔAB]* (lanes *4–6*) transgenic flies. The *top* panel (*SqdB/SqdS*) presents an exposure of the gel six times longer than for the *SqdA* panel to clearly display the weakly expressed *SqdS* transcript in males.

ing proteins may not be required for embryonic patterning but may, rather, be involved in the processing of a variety of host transcripts crucial for cellular viability and/or basic cellular functions.

Biochemical and genetic experiments have shown that PSI contributes to the soma-specific inhibition of *P*-element pre-mRNA splicing by binding to *P*-element exonic sequences (Siebel et al. 1994) and by interacting, through its AB motif, with the *Drosophila* U1 snRNP 70K protein (Labourier et al. 2001). This protein–protein interaction is very specific and, so far, no other PSI-interacting proteins or proteins containing an AB-like motif have been identified in *Drosophila*. The isolation of the recessive lethal *v16* PSI mutant allele gave us the opportunity to examine for the first time the contribution to metazoan development of a direct and specific interaction between a nuclear RNA-binding protein and a constitutive snRNP particle. Although full-length PSI protein is required to fully complement the *v16* mutation, transgenic *Drosophila* in which the only source of PSI protein is the ΔAB domain deletion mutant are viable. This suggests that the four PSI KH domains are necessary and sufficient to rescue *Drosophila* somatic development. The PSI AB motif does not contribute to the specificity and affinity of PSI RNA binding in vitro (Labourier et al. 2001). Thus, the KH domains of PSI may be sufficient to target PSI to pre-mRNA containing high-affinity sequences during specific developmental stages or in specific tissues. In addition, a functional interaction between PSI and U1 snRNP particles, mediated by the PSI AB motif, may be crucial to control the processing of specific PSI-interacting transcripts, essential for a subset of tissue-, stage-, or sex-specific developmental programs.

Consistent with this idea, we found that transgenic *v16;P[PSIΔAB]* males are completely sterile, but their rescued sisters are fertile and lay eggs without apparent abnormalities. Although little data are available, somatic components of the male gonad seem to communicate with the germ line to influence its development. Somatic signals have been suggested to control the self-renewing potential of male germ-line stem cells during spermatogenesis in mammals (Meng et al. 2000) and *Drosophila* (Kiger et al. 2000; Tran et al. 2000). The observation that PSI is highly expressed in both germ-line and somatic cells in testes invites speculation that PSI modulates male-specific somatic or germ-line signals, or a combination of both, that control spermatogenesis. Such signals may be absent or defective in the sterile *v16;P[PSIΔAB]* males.

Because there is almost no postmeiotic transcription during spermatogenesis, RNA-binding proteins involved in nuclear pre-mRNA processing, nucleo–cytoplasmic export, RNA stability, or translation initiation play a crucial role in sperm maturation (Venables and Eperon 1999). PSI is highly expressed in primary spermatocytes and in large mature spermatocytes. It is precisely during this growth and gene expression period that the cells transcribe and process most, if not all, of the gene products needed for the subsequent, major, morphogenetic events of sperm development. An alteration of this critical genetic program in *v16;P[PSIΔAB]* males dramatically affects meiosis and the subsequent spermatid elongation and maturation stages. Lack of the PSI–U1 snRNP association in *v16;P[PSIΔAB]* testes leads to incorrect processing of specific PSI-bound transcripts, such as the *hrp40/squid* mRNA. *squid* is required for dorsoventral axis patterning during *Drosophila* oogenesis, and the different Sqd protein isoforms perform overlapping, but nonequivalent, functions in the localization and translational regulation of specific mRNAs in the female germ line (Kelley 1993; Norvell et al. 1999). Sqd may also play an essential role in the male germ line, and a twofold reduction of SqdA expression in the testes may contribute to the *v16;P[PSIΔAB]* male sterility phenotype. In agreement with this model, the absence of the PSI AB

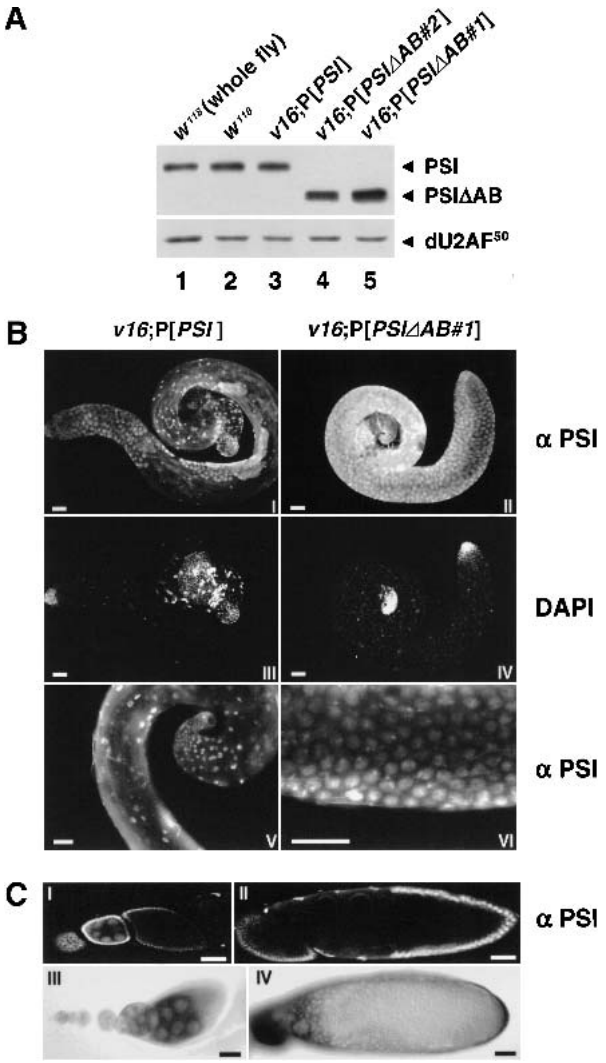

Figure 6. Pattern of PSI expression in *Drosophila* testes and ovaries. (*A*) Immunoblot analyses of testes protein extracts prepared from w^{1118} males (lane *2*) or homozygous *v16* males rescued by the *PSI* (lane *3*) or *PSIΔAB* (lanes *4,5*) cDNA transgenes were performed as in Figure 1B. A w^{1118} whole-fly protein extract was processed in parallel (lane *1*). (*B*) Testes dissected from homozygous *v16* adult males rescued by the *PSI* (*I,III,V*) or *PSIΔAB#1* (*II,IV,VI*) cDNA transgenes were fixed and stained with affinity-purified anti-PSI rabbit antibodies and Alexa Fluor secondary antibodies (*I,II,V,VI*) and with DAPI (*III,IV*). Magnification of the basal end of a *v16;P[PSI]* testis (*V*) or the central part of a *v16;P[PSIΔAB#1]* testis (*VI*) shows the nuclear localization of both the PSI and PSIΔAB proteins in somatic and germ-line cells. Scale bar, 50 µm. (*C*) Stage 4–9 (*I*), 2–8 (*III*), 10 (*II*), or mature (*IV*) oocytes from w^{1118} females were fixed and stained with anti-PSI polyclonal antibodies (*I,II*) or hybridized with a digoxygenin-labeled anti-sense PSI RNA probe (*III,IV*). To observe the very low level of PSI protein expression, whole-mount ovarioles were analyzed by confocal imaging. Scale bar, 50 µm.

motif does not alter the *squid* splicing pattern in ovaries, and oogenesis proceeds normally in *v16;P[PSIΔAB]* females.

Other recessive mutations in genes encoding splicing factors such as the U2AF small or large subunit as well as the SR protein B52 have previously been shown to affect *Drosophila* viability and development (Kanaar et al. 1993; Ring and Lis 1994; Rudner et al. 1996). Yet, it has not been possible to identify splicing defects in these mutants. The fact that *v16;P[PSIΔAB]* males are viable, together with the emergence of new genomic tools, such as DNA microarrays, allowed us to study for the first time an RNA-processing defect at the genome-wide level. By combining large-scale immunopurification experiments with mRNA profiling data, we have been able to identify four categories of transcripts. The first class represents the specific transcripts, such as *yps*, *Hsp60*, *desat1*, and *squid*, that interact with PSI and show altered expression patterns in *v16;P[PSIΔAB]* males. About 20% of the PSI-interacting transcripts belong to this class. This number may be an underestimate because of the stringent filters used to analyze our raw microarray data and to eliminate any putative false-positive candidates (see Materials and Methods). All these transcripts contain short exonic sequences that resemble the high-affinity RNA consensus motif identified by in vitro selection using recombinant PSI protein (RCYYC UURYRC; Amarasinghe et al. 2001) or the RNA sequence bound by PSI within the *P*-element third intron 5′-exon negative regulatory element (AAGUAUAG GUUAAG; Siebel et al. 1994). As previously reported for *P*-element pre-mRNA splicing (Labourier et al. 2001), a direct interaction between PSI and U1 snRNP particles appears to be required for efficient processing of these transcripts in vivo.

Interestingly, the mRNA expression level of 80% of the PSI-interacting targets was not altered in *v16;P[PSIΔAB]* males (see Table 2). Consistent with the observation that the *v16;P[PSIΔAB]* transgenic lines show only subtle developmental defects and are viable, the four PSI KH domains may be sufficient for processing this second class of transcripts. This result fits well with the report that only 5%–10% of the PSI protein present in Kc cell nuclear extracts is found associated with affinity-purified U1 snRNP particles (Labourier et al. 2001).

The third class of transcripts does not interact with PSI, but is differentially expressed in *v16;P[PSIΔAB]* males. These variations may also contribute to the male sterility phenotype. However, we cannot rule out the possibility that these differences are an indirect consequence, rather than the cause, of the *v16;P[PSIΔAB]* phenotype. For example, the underrepresentation of post-meiotic cells in *v16;P[PSIΔAB]* testes might result in a reduced level of expression of specific transcripts in *v16;P[PSIΔAB]* males and account for some of the changes identified in our mRNA profiling experiments (Table 1; Fig. 4A, see the shift toward negative values in the distribution analysis). Finally, and as expected, the vast majority of the cellular transcripts did not show any significant variations between *v16;P[PSI]* and *v16;P[PSIΔAB]* males. This last class represents many negative controls in our microarray experiments and further validates the quality and the reproducibility of our data.

Strikingly, several genes involved in synaptic transmission and axon guidance show altered expression patterns in the *v16;P[PSIΔAB]* mutants (see Table 1). In *Drosophila*, a wide variety of mutations affecting the nervous system have been shown to also alter male courtship behavior. These mutations are almost invariably pleiotropic and affect systems such as learning and memory, vision, olfaction, audition or locomotion, as well as spermatogenesis (Hall 1994; Orgad et al. 1997). For example, a mutation in the *courtless* gene results in a sixfold increase of courtless expression, meiosis defects during spermatogenesis, and male courtship behavior disorders (Orgad et al. 2000). This phenotype is very similar to the v16;P[PSIΔAB] phenotype. No variations in the level of courtless expression were detected in *v16;P[PSIΔAB]* males or females, but courtship behavior was clearly affected in *v16;P[PSIΔAB]* males. It is therefore tempting to propose that PSI may also function in a subset of specific and discrete developmental programs in the nervous system. In agreement with this idea, several targets with altered expression profiles in *v16;P[PSIΔAB]* males (*CG10480*, *CG1782*, *CG8604*, *CG14472*, *CG11172*, and *CG1691*) were recently identified in a gain-of-function screen for genes controlling axon guidance and synaptogenesis in *Drosophila* (Kraut et al. 2001).

Members of the FBP/KSRP family, the mammalian PSI orthologs, are also involved in neuron-specific RNA-processing events. FBP2/KSRP modulates the alternative splicing of the human *src* pre-mRNA in neuronal cells (Min et al. 1997). FBP expression is developmentally regulated and detected only in the brain and testes of adult mouse and chicken (Wang et al. 1998). In addition, FBP specifically binds the 3′ UTR of the human *GAP43* mRNA and has been proposed to modulate its stability during neuronal differentiation (Irwin et al. 1997). PSI and the FBP/KSRP proteins may use similar mechanisms to modulate the processing and/or the stability of specific target transcripts. Future genome-wide studies using improved cDNA microarrays will certainly help to identify the specific sets of genes whose expression is directly regulated by individual RNA-binding proteins in *Drosophila* and humans. These data should provide new insights into how these essential factors contribute to metazoan development according to tissue-, developmental-stage-, or sex-specific cues. Importantly, this knowledge will also help to better decipher the altered RNA-processing patterns characteristic of tumor or disease states in humans.

Materials and methods

Drosophila *stocks and complementation analysis*

For the local transposition/excision screen, the strain l(2)k05207 was crossed to a source of transposase Δ2-3 (*99B*). Three strains, not null for PSI, were identified by darkening of eye color and inverse PCR amplification of genomic regions flanking the novel *P*-element insertions. One strain, #855, had a new *P* element inserted ~2 kb upstream of the *PSI* coding sequence. The original *l(2)k05207 P* element was removed from the #855 strain in a precise excision screen by crossing with the Δ2-3 (*99B*) line, selection of lighter eye color, and PCR analysis. The resulting strain B34, carrying only one *P*-element insertion ~2 kb upstream of the *PSI* coding sequence, was mated to a source of transposase Δ2-3 (*99B*) in a *mus 309* mutant background. *P*-element excision in a *mus309* mutant background yields larger deletions surrounding the *P*-element insertion site (J.W. Feiger and D.C. Rio, unpubl.). Of the 53 putative excision strains analyzed in this imprecise screen, one null mutant was identified and named *v16*. For the rescue experiments, the pw8-PSI genomic plasmid was prepared by ligating a 10.6-kb *Xba*I–*Xba*I fragment from λFIX6a to the transformation vector pw8 linearized with *Xba*I. The λFIX6a clone was isolated from a *Drosophila* genomic library by screening with a *PSI* cDNA probe generated from pNB40 M1 (Siebel et al. 1995) using standard procedures. The pw8-PSI genomic plasmid was linearized at the unique site *Mlu*I (132 nt downstream of the ATG), filled in with Klenow DNA polymerase and religated to create the pw8-PSI genomic frameshift transformation vector. The in vivo PSI expression transformation vectors (*pW8-PSI* cDNA and *pw8-PSIΔAB* cDNA) were prepared by replacing an *Rsr*II–*Hin*dIII fragment within the pw8-PSI genomic plasmid by an *Rsr*II–*Hin*dIII fragment containing *PSI* or *PSIΔAB* cDNA, isolated from pGEM2 PSI or pGEM2 PSIΔAB (Labourier et al. 2001). Germ-line transformation of w^{1118} embryos was carried out using standard microinjection methods. The transposon integration sites were mapped to individual chromosomes using balancer stocks. Crosses were performed on standard cornmeal–agar–molasses medium at 25°C or 18°C. All the lines used in this work are available from our lab stock collection or the *Drosophila* Stock Center at Bloomington, Indiana.

Protein extracts and protein–protein interaction assays

Whole-fly, larva, testis, and embryo protein extracts were prepared as described in Labourier et al. (2001). A second-chromosome balancer (*CyO, pAct-GFP*) and a Leica MZ6 stereomicroscope equipped with a GFP PLUS filter were used to select non-fluorescent homozygous *v16* or *v16;P[PSIΔAB]* embryos or larvae. Affinity selection of U1 snRNP particles and GST fusion protein interaction assays were performed as previously described (Labourier and Rio 2001; Labourier et al. 2001) with 50 or 30 µL of embryonic nuclear extract (protein concentration ~20 mg/mL), respectively. Proteins were resolved on 10% polyacrylamide-SDS gels and analyzed by immunoblot with affinity-purified polyclonal antibodies specific for PSI (Siebel et al. 1995) or dU2AF^{50} (Rudner et al. 1998). Immunoreactive proteins were detected using horseradish peroxidase-conjugated secondary antibodies (Bio-Rad) and the ECL reagent (Amersham).

In situ analyses

Testes and ovaries were hand-dissected in a buffer containing 7.5 mg/mL NaCl and 0.35 mg/mL KCl, washed in PBS, and fixed in 3.7% formaldehyde/PBS (2 × 20 min). Embryos were collected and fixed using standard procedures. RNA probes for in situ analyses were prepared using the plasmid pNB40 M1 (Siebel et al. 1995) and hybridized as described previously (Roche et al. 1995). For antibody staining, samples were washed in PBST (PBS with 0.1% Triton X-100), washed twice (15 min each) in PBS containing 0.5% Triton X-100, washed in PBST, and blocked for at least 2 × 30 min in PBSTBN (PBST with 1% bovine serum albumin and 5% normal goat serum) at room temperature. Samples were incubated at 4°C overnight in PBSTBN with a 1:500 dilution of rabbit anti-vasa antibody (Lasko and Ashburner 1990) or 1:1000 dilution of rabbit anti-PSI antibody (Si-

ebel et al. 1995), washed three times in PBST (15 min each), and incubated in a 1:500 dilution of Alexa Fluor 546 goat anti-rabbit secondary antibody (Molecular Probes) in PBSTBN at room temperature for 3 h. After four washes in PBST (15 min each; 0.5 µg/mL DAPI was included in the second wash when required), samples were mounted in PBS/70% glycerol/1% n-propyl gallate.

Microarrays and RT–PCR analyses

cDNA was produced using standard procedures with 2 µg of polyA$^+$ RNA, random hexamer primers (Roche), Superscript II reverse transcriptase (GIBCO BRL), and amino-allyl dUTP (Sigma), and cleaned with QIAquick columns (QIAGEN) prior to and after labeling in the presence of Cy3 or Cy5 fluorescent dyes (Amersham). Fluorescent cDNAs were mixed, heat-denatured, and hybridized to glass slide *Drosophila* cDNA microarrays (Eisen and Brown 1999; White et al. 1999) at 65°C for 15 h in humidified incubation chambers. Arrays were analyzed with the GenePix 4000 scanner and the GenePix Pro 3.0 software (Axon). Raw data from individual microarrays were filtered with the following parameters: signal at 635 or 532 nm, >1500 quanta, signal/background ratio >3, and spot diameter >40 µm. The calculated 635 nm/532 nm ratios ($\log_2$[Cy5/Cy3]) were normalized with a mean of 0 and a variance of 1 (N[0;1]) to allow comparison among nine independent experiments performed with four independent RNA samples. PSI-interacting RNAs were identified using the same procedure, with total embryonic RNA as the control, Cy3-labeled sample, and five independent experiments. Only the transcripts that were reproducibly detected in at least six among nine (mRNA profiling) or three among five (PSI-interacting) independent experiments were selected for analysis. Immunopurification of RNP complexes from embryonic nuclear extracts using anti-PSI antibodies is described elsewhere (M. Blanchette and D.C. Rio, in prep.). Total RNA from 0- to 2-day-old males, dissected testes, or dissected ovaries was purified using the TRIzol reagent (GIBCO BRL). PolyA$^+$ RNA was isolated using the FastTrack mRNA Isolation Kit (Invitrogen). Quantitative RT–PCR experiments were performed as described in Labourier et al. (2001) with total or polyA$^+$ RNA treated with RQ1 DNase (Promega) and 20 pmole of the appropriate PCR primers. All the RNA samples were quantified using the RiboGreen RNA quantitation reagent (Molecular Probes) and a TD-700 fluorometer (Turner Designs).

Acknowledgments

We thank the Berkeley Drosophila Genome Project for access to their microarray printing facility, S.K. Beckendorf for the polyclonal anti-vasa antibody, and G.M. Rubin for the *Drosophila* genomic library. We also acknowledge M.T. Fuller, P. Tomancak, and P. Spellman for helpful advice. This work was funded by a NIH grant R01GM61987-11 to D.C.R. M.B. was supported by a Human Frontier Science Program long-term fellowship. E.L. was supported by a Philippe Foundation grant and a research fellowship from the Association pour la Recherche sur le Cancer (ARC).

The publication costs of this article were defrayed in part by payment of page charges. This article must therefore be hereby marked "advertisement" in accordance with 18 USC section 1734 solely to indicate this fact.

References

Adams, M.D., Tarng, R.S., and Rio, D.C. 1997. The alternative splicing factor PSI regulates *P*-element third intron splicing in vivo. *Genes & Dev.* **11:** 129–138.

Adams, M.D., Celniker, S.E., Holt, R.A., Evans, C.A., Gocayne, J.D., Amanatides, P.G., Scherer, S.E., Li, P.W., Hoskins, R.A., Galle, R.F., et al. 2000. The genome sequence of *Drosophila melanogaster*. *Science* **287:** 2185–2195.

Amarasinghe, A.K., MacDiarmid, R., Adams, M.D., and Rio, D.C. 2001. An in vitro-selected RNA-binding site for the KH domain protein PSI acts as a splicing inhibitor element. *RNA* **7:** 1239–1253.

Black, D.L. 2000. Protein diversity from alternative splicing: A challenge for bioinformatics and post-genome biology. *Cell* **103:** 367–370.

The *C. elegans* Sequencing Consortium. 1998. Genome sequence of the nematode *C. elegans*: A platform for investigating biology. *Science* **282:** 2012–2018.

Chou, T.B. and Perrimon, N. 1996. The autosomal FLP-DFS technique for generating germline mosaics in *Drosophila melanogaster*. *Genetics* **144:** 1673–1679.

Davis-Smyth, T., Duncan, R.C., Zheng, T., Michelotti, G., and Levens, D. 1996. The far upstream element-binding proteins comprise an ancient family of single-strand DNA-binding transactivators. *J. Biol. Chem.* **271:** 31679–31687.

Duncan, R., Bazar, L., Michelotti, G., Tomonaga, T., Krutzsch, H., Avigan, M., and Levens, D. 1994. A sequence-specific, single-strand binding protein activates the far upstream element of c-*myc* and defines a new DNA-binding motif. *Genes & Dev.* **8:** 465–480.

Eisen, M.B. and Brown, P.O. 1999. DNA arrays for analysis of gene expression. *Methods Enzymol.* **303:** 179–205.

Eperon, I.C., Ireland, D.C., Smith, R.A., Mayeda, A., and Krainer, A.R. 1993. Pathways for selection of 5′ splice sites by U1 snRNPs and SF2/ASF. *EMBO J.* **12:** 3607–3617.

Eperon, I.C., Makarova, O.V., Mayeda, A., Munroe, S.H., Caceres, J.F., Hayward, D.G., and Krainer, A.R. 2000. Selection of alternative 5′ splice sites: Role of U1 snRNP and models for the antagonistic effects of SF2/ASF and hnRNP A1. *Mol. Cell. Biol.* **20:** 8303–8318.

Forch, P., Puig, O., Kedersha, N., Martinez, C., Granneman, S., Seraphin, B., Anderson, P., and Valcarcel, J. 2000. The apoptosis-promoting factor TIA-1 is a regulator of alternative pre-mRNA splicing. *Mol. Cell* **6:** 1089–1098.

Fuller, M.T. 1993. Spermatogenesis in *Drosophila*. In *The development of* Drosophila melanogaster (eds. M. Bate and A. Martinez Arias), pp. 71–148. Cold Spring Harbor Laboratory Press, Cold Spring Harbor, NY.

Graveley, B.R. 2001. Alternative splicing: Increasing diversity in the proteomic world. *Trends Genet.* **17:** 100–107.

Hall, J.C. 1994. The mating of a fly. *Science* **264:** 1702–1714.

Hirose, Y. and Manley, J.L. 2000. RNA polymerase II and the integration of nuclear events. *Genes & Dev.* **14:** 1415–1429.

Irwin, N., Baekelandt, V., Goritchenko, L., and Benowitz, L.I. 1997. Identification of two proteins that bind to a pyrimidine-rich sequence in the 3′-untranslated region of GAP-43 mRNA. *Nucleic Acids Res.* **25:** 1281–1288.

Kanaar, R., Roche, S.E., Beall, E.L., Green, M.R., and Rio, D.C. 1993. The conserved pre-mRNA splicing factor U2AF from *Drosophila*: Requirement for viability. *Science* **262:** 569–573.

Kelley, R.L. 1993. Initial organization of the *Drosophila* dorsoventral axis depends on an RNA-binding protein encoded by the squid gene. *Genes & Dev.* **7:** 948–960.

Kiger, A.A., White-Cooper, H., and Fuller, M.T. 2000. Somatic support cells restrict germline stem cell self-renewal and promote differentiation. *Nature* **407:** 750–754.

Kohtz, J.D., Jamison, S.F., Will, C.L., Zuo, P., Luhrmann, R., Garcia-Blanco, M.A., and Manley, J.L. 1994. Protein–protein interactions and 5′-splice-site recognition in mammalian

mRNA precursors. *Nature* **368:** 119–124.
Kraut, R., Menon, K., and Zinn, K. 2001. A gain-of-function screen for genes controlling motor axon guidance and synaptogenesis in *Drosophila*. *Curr. Biol.* **11:** 417–430.
Labourier, E. and Rio, D.C. 2001. Purification of *Drosophila* snRNPs and characterization of two populations of functional U1 particles. *RNA* **7:** 457–470.
Labourier, E., Adams, M.D., and Rio, D.C. 2001. Modulation of *P*-element pre-mRNA splicing by a direct interaction between PSI and U1 snRNP 70K protein. *Mol. Cell* **8:** 363–373.
Lasko, P.F. and Ashburner, M. 1990. Posterior localization of vasa protein correlates with, but is not sufficient for, pole cell development. *Genes & Dev.* **4:** 905–921.
Lou, H., Neugebauer, K.M., Gagel, R.F., and Berget, S.M. 1998. Regulation of alternative polyadenylation by U1 snRNPs and SRp20. *Mol. Cell. Biol.* **18:** 4977–4985.
Mancebo, R., Lo, P.C., and Mount, S.M. 1990. Structure and expression of the *Drosophila melanogaster* gene for the U1 small nuclear ribonucleoprotein particle 70K protein. *Mol. Cell. Biol.* **10:** 2492–2502.
Matunis, E.L., Matunis, M.J., and Dreyfuss, G. 1992. Characterization of the major hnRNP proteins from *Drosophila melanogaster*. *J. Cell Biol.* **116:** 257–269.
Meng, X., Lindahl, M., Hyvonen, M.E., Parvinen, M., de Rooij, D.G., Hess, M.W., Raatikainen-Ahokas, A., Sainio, K., Rauvala, H., Lakso, M., et al. 2000. Regulation of cell fate decision of undifferentiated spermatogonia by GDNF. *Science* **287:** 1489–1493.
Min, H., Turck, C.W., Nikolic, J.M., and Black, D.L. 1997. A new regulatory protein, KSRP, mediates exon inclusion through an intronic splicing enhancer. *Genes & Dev.* **11:** 1023–1036.
Mount, S.M. and Salz, H.K. 2000. Pre-messenger RNA processing factors in the *Drosophila* genome. *J. Cell Biol.* **150:** F37–F44.
Norvell, A., Kelley, R.L., Wehr, K., and Schupbach, T. 1999. Specific isoforms of squid, a *Drosophila* hnRNP, perform distinct roles in Gurken localization during oogenesis. *Genes & Dev.* **13:** 864–876.
Orgad, S., Rosenfeld, G., Smolikove, S., Polak, T., and Segal, D. 1997. Behavioral analysis of *Drosophila* mutants displaying abnormal male courtship. *Invert. Neurosci.* **3:** 175–183.
Orgad, S., Rosenfeld, G., Greenspan, R.J., and Segal, D. 2000. courtless, the *Drosophila* UBC7 homolog, is involved in male courtship behavior and spermatogenesis. *Genetics* **155:** 1267–1280.
Ring, H.Z. and Lis, J.T. 1994. The SR protein B52/SRp55 is essential for *Drosophila* development. *Mol. Cell. Biol.* **14:** 7499–7506.
Roche, S.E., Schiff, M., and Rio, D.C. 1995. *P*-Element repressor autoregulation involves germ-line transcriptional repression and reduction of third intron splicing. *Genes & Dev.* **9:** 1278–1288.
Rudner, D.Z., Kanaar, R., Breger, K.S., and Rio, D.C. 1996. Mutations in the small subunit of the *Drosophila* U2AF splicing factor cause lethality and developmental defects. *Proc. Natl. Acad. Sci.* **93:** 10333–10337.
———. 1998. Interaction between subunits of heterodimeric splicing factor U2AF is essential in vivo. *Mol. Cell. Biol.* **18:** 1765–1773.
Siebel, C.W., Kanaar, R., and Rio, D.C. 1994. Regulation of tissue-specific *P*-element pre-mRNA splicing requires the RNA-binding protein PSI. *Genes & Dev.* **8:** 1713–1725.
Siebel, C.W., Admon, A., and Rio, D.C. 1995. Soma-specific expression and cloning of PSI, a negative regulator of *P* element pre-mRNA splicing. *Genes & Dev.* **9:** 269–283.
Smith, C.W. and Valcarcel, J. 2000. Alternative pre-mRNA splicing: The logic of combinatorial control. *Trends Biochem. Sci.* **25:** 381–388.
Spingola, M. and Ares, M. 2000. A yeast intronic splicing enhancer and Nam8p are required for Mer1p-activated splicing. *Mol. Cell* **6:** 329–338.
Tran, J., Brenner, T.J., and DiNardo, S. 2000. Somatic control over the germline stem cell lineage during *Drosophila* spermatogenesis. *Nature* **407:** 754–757.
Venables, J.P. and Eperon, I. 1999. The roles of RNA-binding proteins in spermatogenesis and male infertility. *Curr. Opin. Genet. Dev.* **9:** 346–354.
Wang, X., Avigan, M., and Norgren, R.B. 1998. FUSE-binding protein is developmentally regulated and is highly expressed in mouse and chicken embryonic brain. *Neurosci. Lett.* **252:** 191–194.
White, K.P., Rifkin, S.A., Hurban, P., and Hogness, D.S. 1999. Microarray analysis of *Drosophila* development during metamorphosis. *Science* **286:** 2179–2184.